Structural, Morphological, and Magnetic Properties of Nickel Substituted Cobalt Zinc Nanoferrites at Different Sintering Temperature

D. Parajuli, N. Murali and K. Samatha

Journal of Nepal Physical Society

Volume 7, Issue 2, June 2021

ISSN: 2392-473X (Print), 2738-9537 (Online)

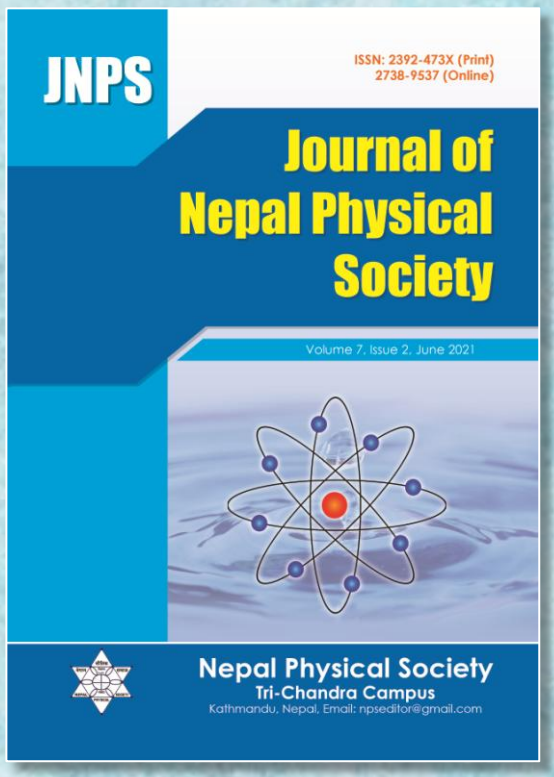

JNPS, **7** (2), 24-32 (2021)

DOI: https://doi.org/10.3126/jnphyssoc.v7i2.38619

Published by:

Nepal Physical Society

P.O. Box: 2934

Tri-Chandra Campus

Kathmandu, Nepal

Email: nps.editor@gmail.com

JNPS 7 (2): 24-32 (2021)
ISSN: 2392-473X (Print), 2738-9537 (Online)

Research Article *© Nepal Physical Society*
DOI: https://doi.org/10.3126/jnphyssoc.v7i2.38619

Structural, Morphological, and Magnetic Properties of Nickel Substituted Cobalt Zinc Nanoferrites at Different Sintering Temperature

D. Parajuli[1, 2, *], N. Murali[3] and K. Samatha[2]

[1] Research Center for Applied Science and Technology, Tribhuvan University, Kathmandu, Nepal

[2] Department of Physics, College of Science and Technology, Andhra University, Visakhapatnam, India

[2] Department of Engineering Physics, College of Engineering (A), Andhra University, Visakhapatnam, India

[*]Corresponding Email: deepenparaj@gmail.com

Received: *13 April, 2021;* ***Revised:*** *10 May, 2021;* ***Accepted:*** *27 June, 2021*

ABSTRACT

Co-precipitation was used for the preparation of $Co_{0.5-x}Ni_xZn_{0.5}Fe_2O_4$ (x = 0 to 0.3) nanoferrites. The inverse spinel structure of the samples was clearly shown by the structural analysis of X-ray Diffractometer (XRD) and Fourier Transform Infrared (FTIR) Spectroscopy. We have studied the effect of sintering temperature (500^{o}C) on the lattice constant and particle size using XRD. The average lattice parameters for the non-sintered and sintered samples were 8.377 Å and 8.354 Å respectively. For the non-sintered sample, the nickel concentration decreases the lattice parameter from 8.354 Å to 8.310 Å due to its smaller ionic radii than that of cobalt. While for a sintered sample at 500^{o}C, the lattice parameter increases for concentration x=0.3 due to the thermal effect. The particle size calculated by Transmission Electron Microscope (TEM) agrees well with that of XRD. The morphological and compositional analysis was done with the help of Scanning Electron Microscopy (SEM) and the attached Energy Dispersive X-ray (EDX) Analyzer. The increasing percentage of nickel with decreasing percentage of cobalt shows that the cobalt is substituted by Nickel. The magnetic properties were studied by Vibrational Spectrometer (VSM). The value of saturation magnetization is higher for x=0.1 but lower for x=0.2 and 0.3 due to their particle size. The hysteresis loop of the samples their superparamagnetic behavior at room temperature.

Keywords: Co-precipitation, Inverse spinel ferrite, Thermal effect, Superparamagnetic.

1. INTRODUCTION

Cobalt ferrites are mixed hard ferrite having an inverse spinel structure. They are physically and chemically stable with a higher value of coercivity. This is why they are used for magnetic recording systems. Smaller grain sizes are mostly preferable for recording media. But, these sizes produce instability in a magnetic property. This problem can be solved by synthesizing ferrites particles with homogeneous magnetic particles. Cobalt Zinc ferrite is one of them that can be used as inducing material in electromagnetic devices. Ferrites with single-phase and smaller size magnetic materials can be prepared in a controlled way by precipitation with the reverse micelles method. There are many other methods for bulk ferrites including ceramic methods etc. Laser irradiation [1], chemical co-precipitation method [2], the hydrothermal method [3], and co-precipitation method [4] were used in the past and showed that a higher amount of zinc gives superparamagnetic and lower gives ferromagnetic nature to the material. Likewise, magnetization decreases with increasing particle size. The addition of cobalt with zinc shows more improvement in magnetic property in the nanoscale [5]. A higher amount of Zn in the Co-Zn system decreases the saturation magnetization [6, 7] in ceramic techniques. The sintering temperature also affects the permittivity of the ferrite material, however, permeability is affected by both frequency and sintering temperature [8]. In the same way, their dielectric behavior is also

dependent on temperature and frequency [9]. The hopping mechanism gives their electrical conductivity. The superparamagnetic relaxation is also observed in chromium substituted cobalt zinc ferrites. Omprakash *e.al.* 2007 found that the magnetic saturation was decreased for the increased value of annealing temperature on Nickel substituted cobalt Zinc ferrite [10]. The reason behind this was the superparamagnetic phase variation and redistribution of cations. The size of the nanoparticles affects the value of coercivity like antibacterial properties in ZnO and CdO nanoparticles [11][12].

Recently, we have studied the structural and morphological properties of Cu substituted Ni/ Zn in NiZn ferrites [13][14], microstructural, thermal, electrical, and magnetic analysis of Mg^{2+} substituted Cobalt ferrite [15], Cr substitution effect on magnetic properties of Co-Cu nano ferrites [16], Magnetic and DC electrical resistivity properties of Cu doped $Mg_{0.\ 6-x}Ni_{0.\ 4}CuxFe_2O_4$ ferrite [17], magnetic and DC electrical properties of Cu doped Co-Zn nanoferrites [18], Cr^{3+} substitution effect on dc electrical resistivity and magnetic properties of $Cu_{0.7}Co_{0.3}Fe_{2-x}Cr_xO_4$ ferrite nanoparticles prepared by sol-gel auto combustion method [19], DC electrical resistivity and magnetic properties of Co substituted NiCuZn nanoferrites [20], cadmium substitution effect on structural, electrical and magnetic properties of Ni-Zn nanoferrites.[21], Cu substitution effect on the structural, magnetic, and dc electrical resistivity response of $Co_{0.5}Mg_{0.5-x}Cu_xFe_2O_4$ nanoferrites[22], Cu substitution effect on magnetic and DC electrical resistivity properties of Ni-Zn nanoferrites [23], and Cu substitution effect on magnetic properties of $Co_{0.6}Ni_{0.4}Fe_2O_4$ nanoferrites [24]. It is found that they all have satisfied their respective spinel structures as nanoferrites with several other properties and found more useful than the traditional compositions in daily applications as we pronounce that for ferrites.

More details about the effects made by nickel substitution on $Co_{0.5}Zn_{0.5}Fe_2O_4$ are reported in this paper.

2. MATERIAL AND METHODS

The composition varying from x=0.0 to 0.3 for $Co_{0.5-x}Ni_xZn_{0.5}Fe_2O_4$ nanoparticles are synthesized by the co-precipitation method. Ferric chloride, Zinc Sulphate, Cobalt Chloride, and Nickel Chloride with molecular formula $FeCl_3$, $ZnSO_4.7H_2O$, $CoCl_2.6H_2O$, and $NiCl_2.6H_2O$ respectively are taken in the appropriate ratio. We have prepared a 100 ml solution containing (0.5-x) mole of cobalt chloride, (x) mole of nickel chloride, 0.5 moles of Zinc Sulphate, and 100 ml of 2 moles of Ferric chloride. They were mixed homogeneously by a magnetic stirrer at 80°C and mixed into the boiling solution of sodium chloride having 0.55 mole in 1330ml pure water to make the pH value 12 during the reaction at 100°C for an hour. In this process, the metal salts are changed to respective hydroxides and then to nanoferrites. The product is centrifuged, washed, dried at room temperature, and grounded on agate mortar to form a pallet pressed under 5 tons for about 3 min. The pallet and powder were sintered at 500°C for two hours and used for characterization of their structural and magnetic properties using X-Ray Diffraction (XRD- Rigaku Miniflex II), Fourier Transform Infrared (FTIR- Perkin-Elmer Rx1) Spectroscopy, Scanning Electron Microscope (SEM- TESCAN, MIRA II LMH) with attached EDX- Inca Oxford, Transmission Electron Microscope (TEM- Hitachi H-8100), and Vibrational Spectromagnetometer (VSM- EZ) for their structural, morphological and magnetic properties.

3. RESULTS AND DISCUSSION

XRD analysis

The powder XRD pattern of $Co_{0.5-x}Ni_xZn_{0.5}Fe_2O_4$ (where x = 0 to 0.3) are shown in figure 1. They show single-phase spinel ferrite. Wider peaks indicate the smaller size of the ferrite particles. The indexing pattern and refining data were done by using Powder-X Indexing Software [25]. The maximum peak (311) indicating the maximum intensity was used for the calculation of crystallite size using Scherrer's formula [26].

$$D_{311} = \frac{k\lambda}{\beta\ cos\theta}$$

where 'k' is the Scherrer's constant, 'λ' is the wavelength of X-ray used, 'β' is the full width at half maxima 'θ' is the Bragg's angle.

The lattice constant and the crystallite size calculated are listed in table 1. The sintering affects greatly in the lattice parameters. The value of as prepared and sintered samples are found to be 8.354 Å and 8.377 Å respectively that are in agreement with previous literature [27].

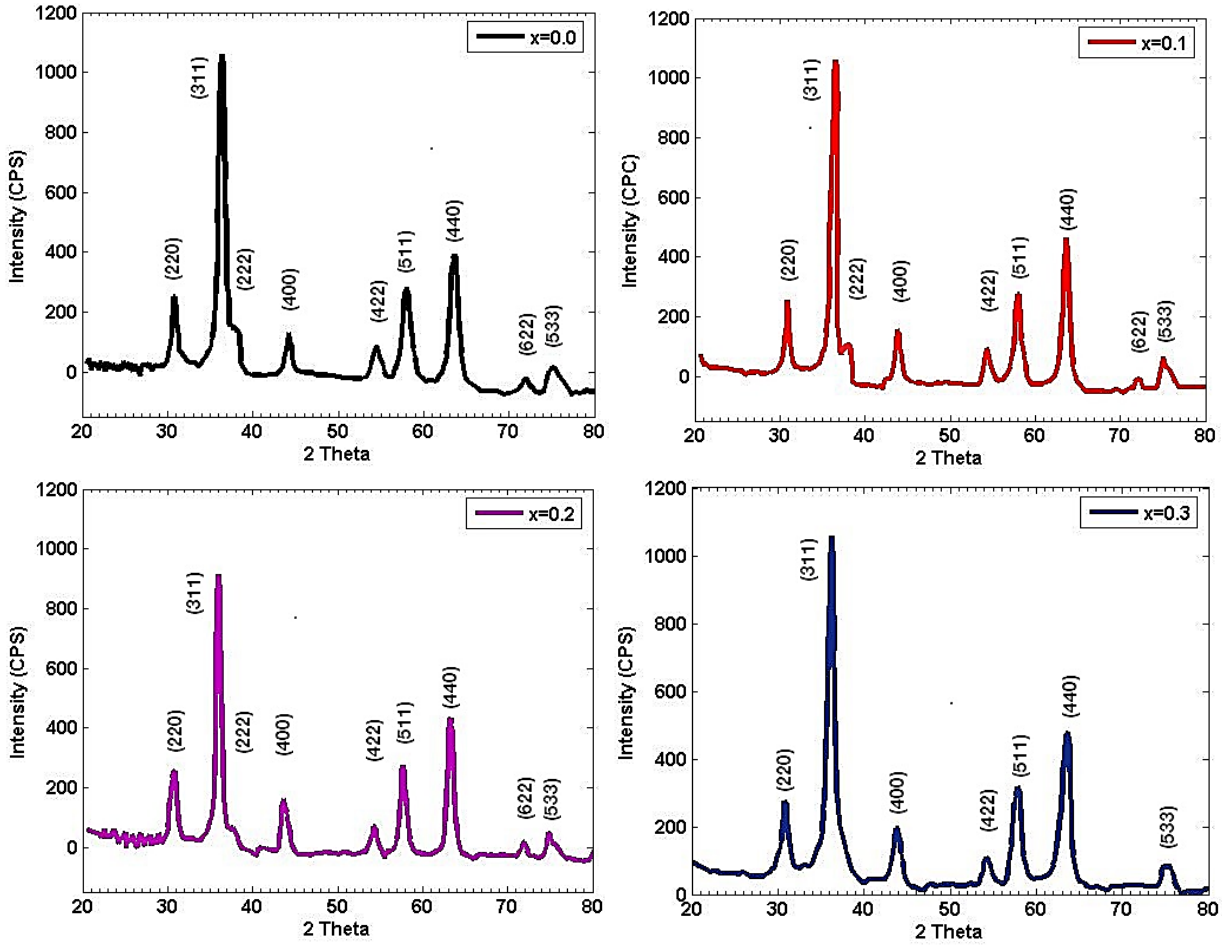

Fig. 1: Powder XRD pattern of $Co_{0.5-x}Ni_xZn_{0.5}Fe_2O_4$ (where x = 0 to 0.3)

Transmission Electron Microscopy (TEM)

The TEM image of $Co_{0.5-x}Ni_xZn_{0.5}Fe_2O_4$ for x=0.2 revealing particle size and morphology with resolution 50 nm (left) and 5 nm (right) are shown in figure 2. The particles seem spherical with an average size of 15nm which agrees with XRD data.

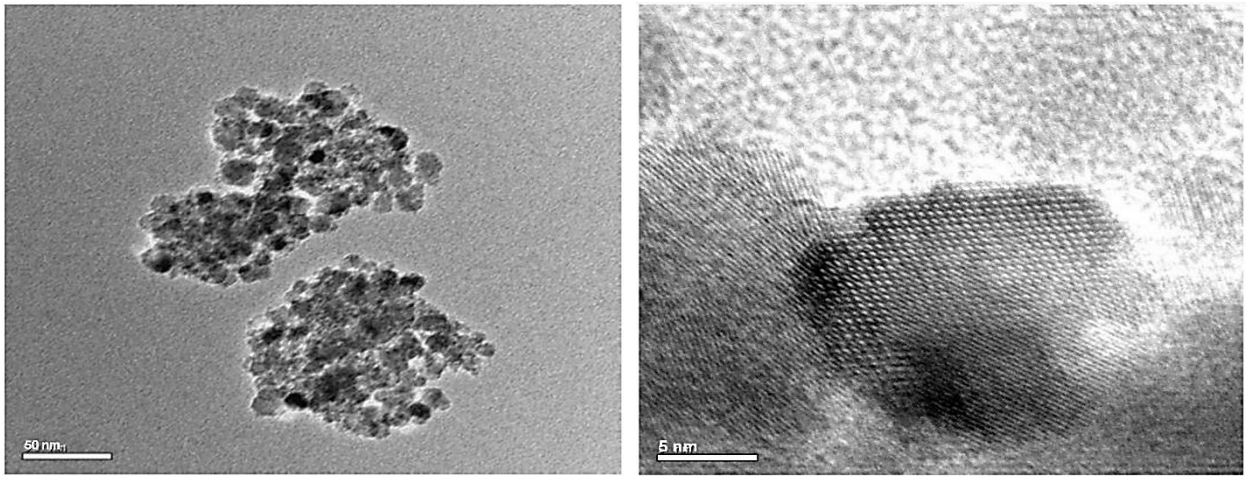

Fig. 2: TEM image of $Co_{0.5-x}Ni_xZn_{0.5}Fe_2O_4$ for x=0.2 with resolution 50 nm (left) and 5 nm (right)

Scanning Electron Microscopy and Energy Dispersive X-ray (SEM with EDX)

The surface morphology and compositional analysis of $Co_{0.5-x}Ni_xZn_{0.5}Fe_2O_4$ are studied with the help of SEM-EDX. The SEM images of the sample with respective compositions are shown in figure 3. The weight percentage of cobalt and nickel in the sample was 14.73, 12.34, 9.93, 7.92 and 1.99, 4.01, 6.42, respectively calculated by EDX. It clearly shows the cobalt is decreasing and nickel is increasing in amount while that for Iron and Zinc are almost unaltered. The substitution element Nickel is be seen in the composition form $Co_{0.5-x}Ni_xZn_{0.5}Fe_2O_4$ (x = 0 to 0.3) as shown in figure 4.

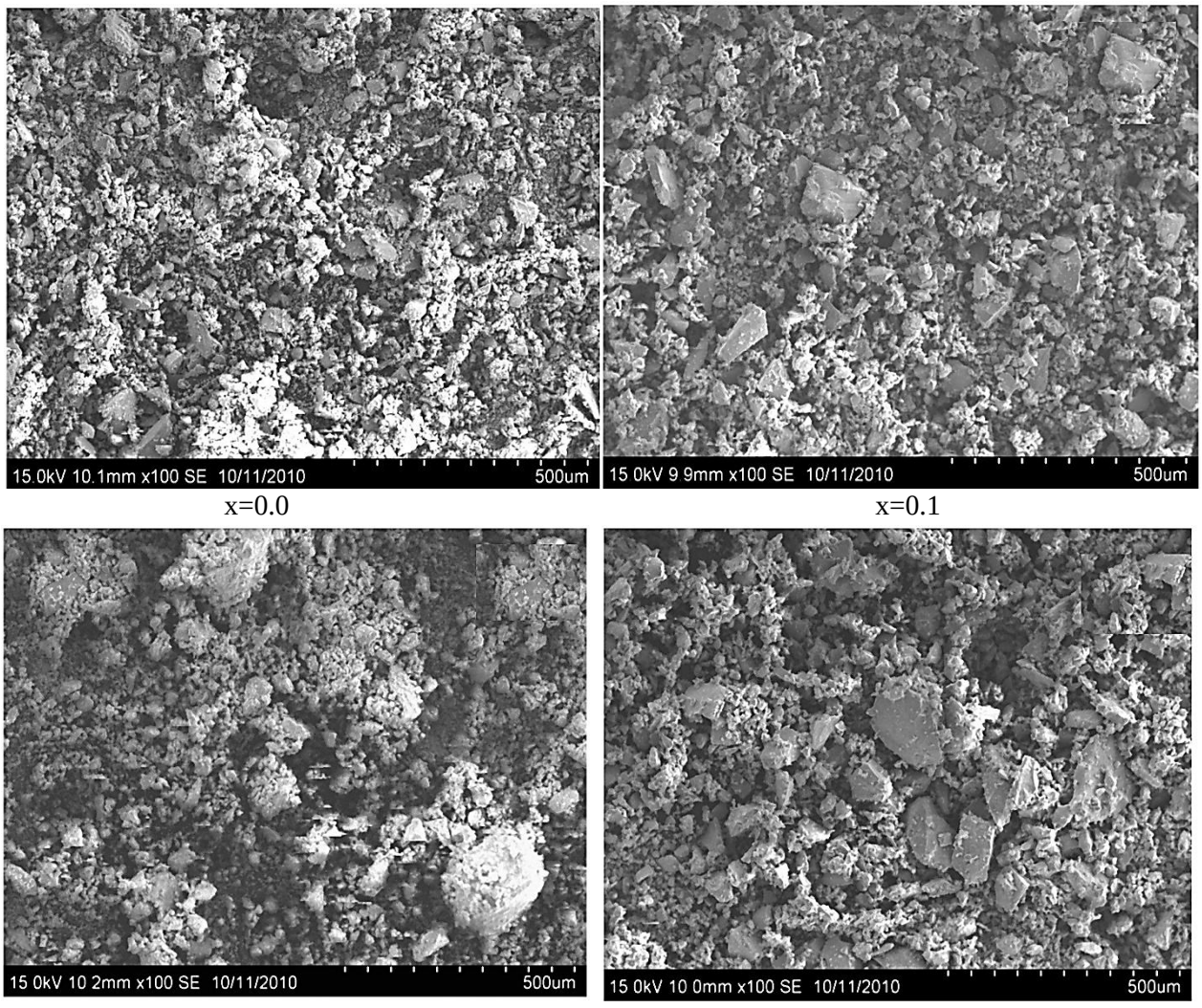

Fig. 3: SEM images for $Co_{0.5-x}Ni_xZn_{0.5}Fe_2O_4$ (x = 0 to 0.3).

The lattice parameter is less for nanosize ferrites (8.356 Å) [28] than that for Bulk (8.37 Å) [29]. This is mainly due to altered cation distribution in nanopowders. In bulk, Zn and Co occupy A and B sites respectively which are altered in nanosize. This pushes Fe^{3+} to the tetrahedral site from its chemically preferable octahedral site. As Fe^{3+} has a smaller ionic radius (0.64Å) and is replacing the divalent cation with larger ionic radii, the lattice parameter decreases in nanoferrite than that in bulk [30, 31]. The increase or decrease in lattice parameter depends not only on temperature but also on cation stoichiometry. If nickel (0.69 Å) substitutes cobalt (0.72 Å), the lattice parameter increases. This is according to Vegard's law [32]. However, in the sintered sample at concentration x=0.3, the lattice parameter is increased due to the formation of Fe^{2+} in the octahedral sites as its ionic radius (0.74 Å) is larger than Fe^{3+} ion (0.64 Å).

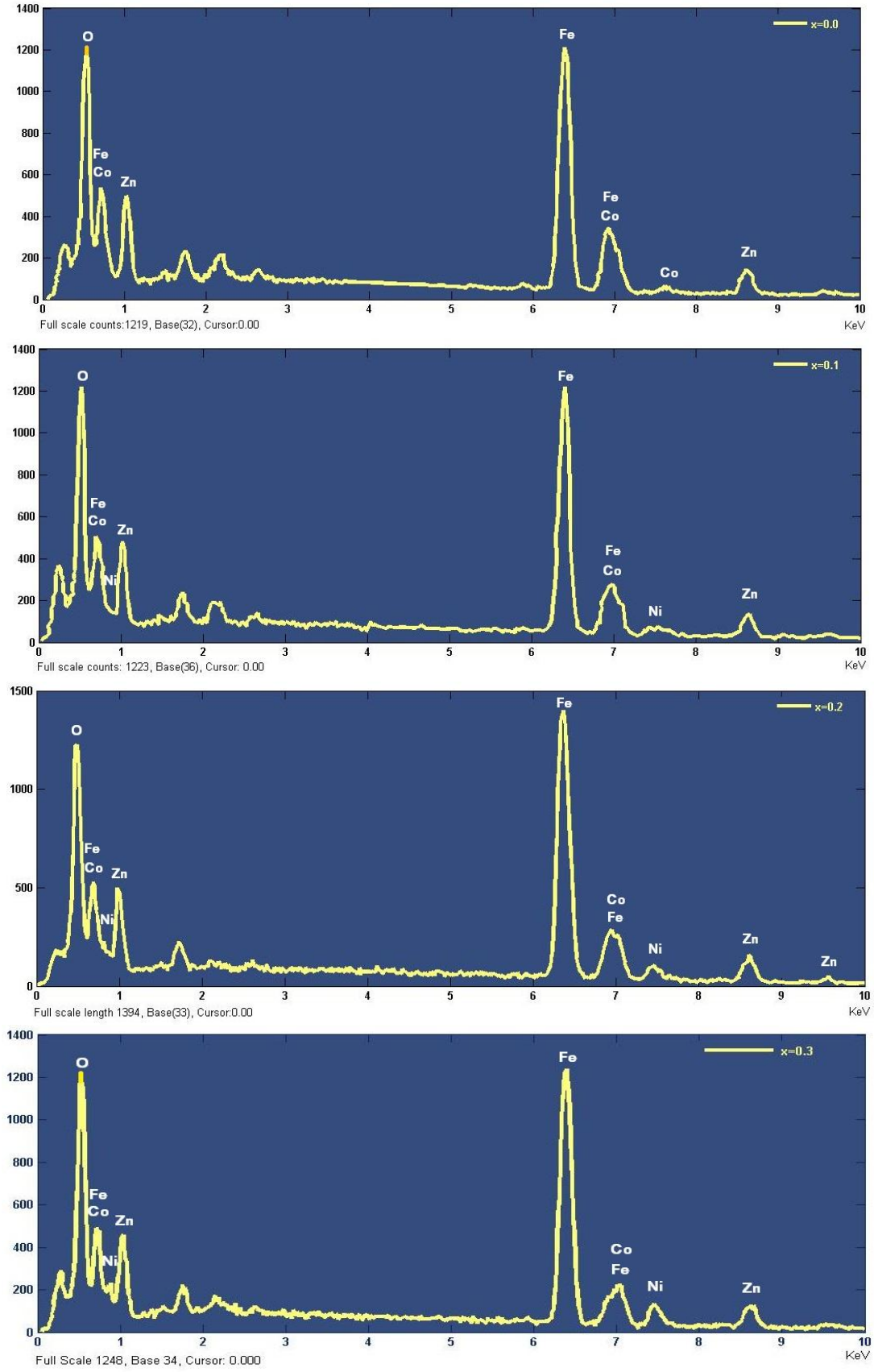

Fig. 4: EDX images of $Co_{0.5-x}Ni_xZn_{0.5}Fe_2O_4$ (x = 0 to 0.3)

Table 1: Structural and magnetic parameters of $Co_{0.5-x}Ni_xZn_{0.5}Fe_2O_4$ (x = 0 to 0.3)

Composition (x)	Average particle size 't'nm		Lattice constant 'a'(A^o)		Saturation Magnetization at 15 kOe (emu/g)
	As prepared sample	Sintered sample at 500°C	As prepared sample	Sintered sample at 500°C	
0	12	16	8.354	8.377	46
0.1	11	15.5	8.333	8.355	30
0.2	14	15	8.329	8.342	40
0.3	15	15.5	8.310	8.349	72

Fourier Transform Infrared (FTIR) Spectra

FTIR spectra of the as-prepared compositions $Co_{0.5-x}Ni_xZn_{0.5}Fe_2O_4$ (x = 0 to 0.3) are shown in figure 5. Due to the two interstitial sites (tetrahedral sites-A, octahedral-B) in the ferrite structures, they have two absorption bands in the range 400-600 cm^{-1}. In this study, the two absorption bands are at 550–600 cm^{-1} (tetrahedral) and 420-450 cm^{-1} (octahedral) [33] respectively indicating ferrites structures. The absorption is due to the metal-oxygen bonds in the respective sites.

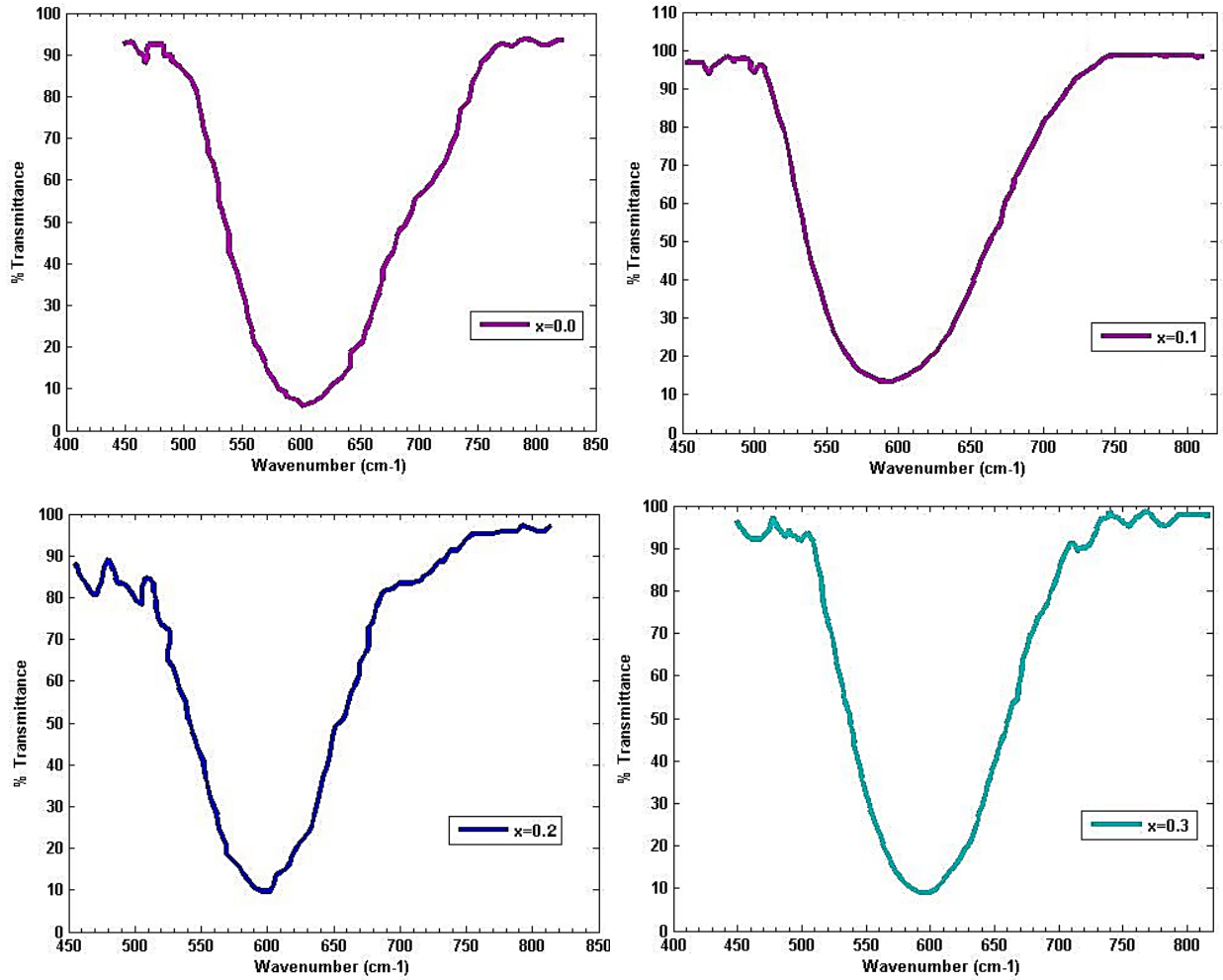

Fig. 5: FTIR spectra for $Co_{0.5-x}Ni_xZn_{0.5}Fe_2O_4$ (x = 0 to 0.3)

VSM Study

The variation of magnetization due to the applied magnetic field for our samples $Co_{0.5-x}Ni_xZn_{0.5}Fe_2O_4$ (x = 0 to 0.3) at 300K is shown in figure 6. The values of magnetization for different concentrations at applied field 15kOe are listed in table 1.

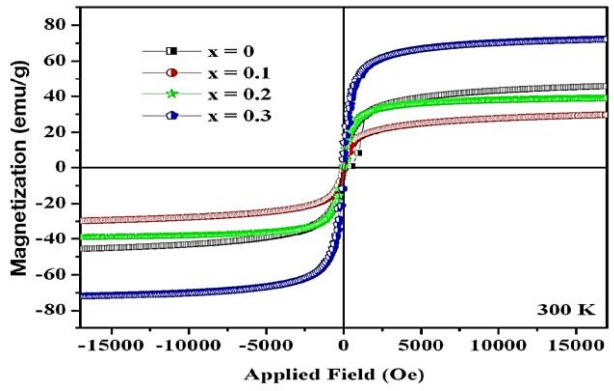

Fig. 6: Hysteresis loop for the compound for $Co_{0.5-x}Ni_xZn_{0.5}Fe_2O_4$ (x = 0 to 0.3) at 300K

On the application of the magnetic field, the magnetization increases as usual. The saturation magnetization decreases with the Nickel concentration and increases with cobalt concentration i.e. it decreases from 49.6 to 33.3 emu/g for x=0.1 and increases from 33.3 emu/g to 74.2 emu/g for x = 0.2 and 0.3. As the Nickel concentration increases at the Cobalt site, the saturation magnetization decreases for x=0.1. As the concentration increases, the decreased magnetic moment in the B site, makes the Fe^{3+} ion moves from A to B site. The A-site cations interaction increases. As the total magnetic moment is $|M_B - M_A|$, the spin canting in the B site increases. This increases the particle size. This result is in good agreement with previous literature [9, 32]. Even after the application of higher magnetic fields in the order of 50 kOe, saturation magnetization sometimes becomes too hard to obtain. This may be due to the difference in spin behavior in the surface and core of the material. The spins are ferromagnetically oriented in the core and are not in order on the surface. They are tilted in random or called random canting. The applied field effect on the surface resulting in slow magnetization due to the disordered spin. The random tilting or canting of the spin bulk [33]. The improved magneto-crystalline-anisotropy of randomly distributed nanoparticles has affected negatively magnetic saturation [20]. The hysteresis loop of $Zn_{0.5}Co_{0.5}Fe_2O_4$ and $Ni_{0.1}Zn_{0.5}Co_{0.4}Fe_2O_4$ shown in the figure revealed that they have neither coercivity nor coercivity. This indicates that they have superparamagnetic behavior at room temperature [35]. Coercivity decreases with increasing temperature. Below blocking temperature, the hysteresis loop exists and above it, the loop vanishes [36]. The increase in coercivity with concentration shows the irreversible domain moment.

3. CONCLUSION

The $Co_{0.5-x}Ni_xZn_{0.5}Fe_2O_4$ (x = 0 to 0.3) nanoferrites were prepared successfully by the co-precipitation method. The structural analysis by XRD and FTIR show their single-phase inverse spinel structure. The average lattice parameters for the non-sintered and sintered samples were 8.377 Å and 8.354 Å respectively. The nickel concentration decreases the lattice parameter from 8.354 Å to 8.310 Å due to its smaller ionic radii than that of cobalt for the non-sintered sample. While for the sintered sample at 500°C, the lattice parameter increases for concentration x=0.3. The reason behind this is the formation of Fe^{+2} (0.74 Å) from F^{+3} (0.64 Å) in the tetrahedral site by thermal effect. The particle size calculated by TEM agrees well with that of XRD. The morphological and compositional analysis was done with the help of SEM attached with EDX. The increasing percentage of nickel with decreasing percentage of cobalt shows that the cobalt is substituted by Nickel. Particle size is found to depend directly on saturation magnetization. So, the value of saturation magnetization given by VSM is higher for x=0.1 but lower for x=0.2 and 0.3. The negligible value of both coercivity and retentivity the superparamagnetic behavior of the samples at room temperature.

REFERENCES

[1] Tawfik, A.; Hamada, I. M. and Hemeda, O. M. "Effect of laser irradiation on the structure and electromechanical properties of Co-Zn Ferrite", *Journal of Magnetism and Magnetic Materials*, **250**: 77-82. (2002).

[2] Gul, I. H.; Abbasi, A. Z., Amin, F.; Anis ur Rehman, M. and Masood, M. "Structural magnetic and electrical properties of Co1-xZnxFe2O4 synthesized by co-precipitation method", *Journal of Magnetism and Magnetic Materials*, **311**: 494–499 (2007).

[3] Gozuak, F.; Koseoglu, Y.; Baykal, A. and Kavas, H. "Synthesis and characterization of CoxZn1-xFe2O4 magnetic nanoparticles via a

PEGassisted route", *Journal of Magnetism and Magnetic Materials*, **321**: 2170-2177 (2009).

[4] Dey, S. and Ghose, J. "Synthesis, Characterization and Magnetic Studies on Nanocrystalline Co0.2Zn0.8Fe2O4", *Materials Research Bulletin*, **38**(11-12): 1653-1660 (2003).

[5] Arulmurugan, R.; Jeyadevan, B.; Vaidyanathan, G. and Senthilnathan, S. "Effect of zinc substitution on Co-Zn and Mn-Zn ferrite nanoparticles prepared by co-precipitation", *Journal of Magnetism and Magnetic Materials*, **288**: 470-477 (2005a).

[6] Islam, M. U.; Rana, M. U. and Abbbas, T. "Study of magnetic interactions in Co-Zn-Fe-O System", Materials Chemistry and Physics, **57**: 190- 193, (1998).

[7] Waje, S. B.; Hashim, M.; Yousoff, W. D. W. and Abbas, Z. "Sintering temperature dependence of room temperature magnetic and dielectric properties of Co0.5Zn0.5Fe2O4 prepared using mechanically alloyed nanoparticles", *Journal of Magnetism and Magnetic Materials*, **322**: 686-691 (2010).

[8] Josyulu, O. S. and Sobhanadri J. "D.C conductivity and dielectric behavior of cobalt-zinc ferrites", *Physica Status Solidi (a)*, **59**: 323-329 (1980).

[9] Sharma, R. K.; Suwalka., O. P.; Lakshmi, N.; Venugopala, K.; Banerjee, A. and Joy, P. A. "Synthesis of chromium substituted nanoparticles of cobalt zinc ferrites by co-precipitation", *Materials Letter*, **59**: 3402-3405 (2005).

[10] Suwalka, O. P.; Sharma, R. K.; Sebastian, V.; Lakshmi, N. and Venugopalan, K. "A study of nanosized nickel substituted Co–Zn ferrite prepared by coprecipitation", *Journal of Magnetism and Magnetic Materials*, **313**(1): 198-203 (2007).

[11] Gudla, U. R.; Parajuli, D.; Suryanarayana, B.; Murali, N.; Raghavendra, V.; Emmanuel, K. A.; Teddesse, P.; Naidu, C. B.; Ramakrishna, Y.; Chandramouli, K.; Samatha, K. "Optical and Luminescence properties of pure, iron-doped and glucose capped ZnO nanoparticles." *Results in Physics*, **19**: 103508 (2020).

[12] Gudla, U. R.; Parajuli, D.; Suryanarayana, B.; Raghavendra, V.; Nandigam, M.; Dominic, S.; Ramakrishna, Y.; Chandramouli, K. Structural, Optical and Luminescence Properties of Pure, Fe doped and Capped CdO Semiconductor nanoparticles for their Antibacterial activity. Journal of Materials Science: *Materials in Electronics*, **32** (25): 3920-3928 (2021).

[13] Parajuli, D. and Samatha K. Structural Analysis of Cu substituted Ni/ Zn in NiZn ferrites. Journal of Physical Science, *BIBECHANA*, **18**(1): 128-133 (2020).

[14] Parajuli, D. and Samatha, K. Morphological Analysis of Cu substituted Ni/ Zn in NiZn ferrites. Journal of Physical Science, *BIBECHANA*, **18** (2): 80-86 (2021).

[15] Mercy, S. J.; Parajuli, D.; Murali, N.; Ramakrishna, A.; Ramakrishna, Y.; Veeraiah, V.; Samatha, K. Microstructural, thermal, electrical and magnetic analysis of Mg^{2+} substituted Cobalt ferrite, *Applied Physics A*, 126-873 (2020).

[16] Phanidhar Varma, P. V. S. K.; Suryanarayana, B.; Raghavendra, V.; Parajuli, D.; Murali, N.; Chandramoli, K. Effect of Cr substitution on magnetic properties of Co-Cu nano ferrites, *Solid State Technology*, **63** (5): 8820-8827 (2020).

[17] Murali, N.; Parajuli, D.; Ramakrishna, A.; Rao, P. S. V. S.; Rao, M. P. Magnetic and DC Electrical Resistivity Properties of Cu doped $Mg_{0.\ 6-x}Ni_{0.\ 4}Cu_xFe_2O_4$ Ferrite, Solid State Technology, **63** (5): 4069-4077 (2020).

[18] Himakar, P.; Parajuli, D.; Murali, N.; Veeraiah, V.; Samatha, K. Tulu Vegayehu Mammo, Mujasam Batoo Khalid, Hadi Muhammad, Raslan Emad, and Syed Farooq, *Magnetic and DC Electrical Properties of Cu Doped Co-Zn Nanoferrites*. *Journal of Electronic Ma. erials*, **50** (6): 3758 (2021).

[19] Chandramouli, K.; Suryanarayana, B.; Phanidhar Varma, P. V. S. K.; Raghavendra, V.; Emmanuel, K. A.; Taddesse, P.; Murali, N.; Wegayehu Mammo, T.; Parajuli, D. Effect of Cr3+ substitution on dc electrical resistivity and magnetic properties of $Cu_{0.7}Co_{0.3}Fe_{2-x}Cr_xO_4$ ferrite nanoparticles prepared by sol-gel auto combustion method, *Results in Physics*, **24** (11): 104117 (2021).

[20] Jayadev, M. K.; Raju, K.; Murali, N.; Parajuli, D.; Samatha, K. DC Electrical Resistivity and Magnetic Properties of Co Substituted NiCuZn Nano Ferrite, Research Square, 1-16 (2021).

[21] Parajuli, D.; Raghavendra, V.; Suryanarayan, B.; Rao, P. A.; Murali, N.; Phanidhar Varma, P.V. S. K.; Giri, R. P.; Ramakrishna, Y.; Chandramouli, K. Taddesse Paulose. *Cadmium substitution effect on structural, electrical, and magnetic properties of Ni-Zn nanoferrites*. *Results in Physics*, **19**: 103947 (2021).

[22] Himakar, P.; Jayadev, K.; Parajuli, D.; Murali, N.; Taddesse, P. Mulushoa, S. Y.; Mammo, T. W.; Kishore Babu, B.; Veeraiah, V.; Samatha, K. Effect *of Cu substitution on the structural, magnetic, and dc electrical resistivity response of Co0.5Mg0.5-xCuxFe2O4 nanoferrites*. *Applied Physics A*, **127**: 371 (2021).

[23] Chandramouli, K.; Rao, P. A.; Suryanarayana, B.; Raghavendra, V.; Mercy, S. J.; Parajuli, D.; Taddesse, P.; Mulushoa, S. Y.; Mammo, T. W.

and Murali, N. Effect of Cu substitution on magnetic and DC electrical resistivity properties of Ni–Zn nanoferrites. *J Mater Sci: Mater Electron* **32:** 15754–15762 (2021).

[24] Ramanjaneyulu, K.; Parajuli, D.; Suryanarayana, B.; Raghavendra, V.; Murali, N.; Chandramouli, K. Synthesis, microstructural and magnetic properties of Cu doped Mg0.5Zn0.5Fe2O4 ferrites. *Solid State Technology*, **64** (2): 7192–7200 (2021)**.**

[25] Dong, C. "POWDERX: Windows-95 based program for powder X-ray diffraction data processing", *Journal of Applied Crystallography*, **32**: 838 (1999).

[26] Cullity, B. D. "Elements of X-ray Diffraction", Addison-Wesley Publishing Co. Inc., 1959.

[27] Arulmurugan, R.; Vaidyanathan, G.; Sendhilnathan, S. and Jeyadevan, B. "Thermomagnetic properties of Co1-xZnxFe2O4 (x=0.1 0.5) nanoparticles", *Journal of Magnetism and Magnetic Materials*, **303**: 131-137(2005b).

[28] Pandya, P. B.; Joshi, H. H. and Kulkarani, R. G. "Bulk magnetic properties of Co-Zn ferrites prepared by co-precipitation method", *Journal of material sciences*, **26**: 5509-5512 (1991).

[29] Upadhyay, C.; Verma, H. C. and Anand, S. "Cation distribution in nanosized Ni–Zn ferrites", *Journal of applied physics*, **95**: 5746-5852 (2004).

[30] Denton, A. R. and Ashcroft, N. W. "Vegard's law", *Physics Review A*, **43**: 3161-3164 (1991).

[31] Waldron, R. D. "Infrared spectra of ferrites", *Physical Review*, **99**: 1727-1735 (1955).

[32] Ichiyanagi, Y.; Uehashi, T.; Yamada, S.; Kanazawa, Y. and Yamada, T. "Thermal fluctuation and magnetization of Ni-Zn ferrite nanoparticles by particle size", *Journal of Thermal Analysis and Calorimetry*, **81**: 541-544 (2005).

[33] Coey, J. M. D. "Noncollinear spin arrangement in ultrafine ferrimagnetic crystals", Vol. 140, *Physical Review Letters*, **27**: 1140-1142 (1971).

[34] Pankhurst, Q. A. and Pollard, R. J. "Origin of the spin-canting anomaly in small ferromagnetic particles", *Physical Review Letters*, **67**: 248-250 (1991).

[35] Tomar, M. S.; Singha, S. P.; Perales-Perezb, O.; Guzmana, R. P.; Calderonc, E. and Rinaldi-Ramos, C. "Synthesis and magnetic behavior of nanostructured ferrites for spintronics", *Microelectronics Journal*, **36**: 475-478 (2005).

[36] Seema Verma Hari, S.; Potdar Sadgopal, K. D. and Joy, P. A. "Synthesis of superparamagnetic magnesium ferrite nanoparticles by microwave-hydrothermal method", *Materials Research Society*, **818**: M5.7.1-7.6. (2004).